Hindawi
Shock and Vibration
Volume 2021, Article ID 2689960, 12 pages
https://doi.org/10.1155/2021/2689960

Research Article

Analysis of Contact Characteristics of Carbon Brush/Slip Ring under Eccentric Oscillation of Hydrogenerator Rotor

Xinze Zhao, Yunfeng Nie, Ming Chen, Hongling Qin, and Xiang Xu

China Three Gorges University, Yichang 443002, China

Correspondence should be addressed to Xiang Xu; xiang_xu@ctgu.edu.cn

Received 22 July 2021; Revised 5 September 2021; Accepted 27 September 2021; Published 21 October 2021

Academic Editor: Zhaoye Qin

In this paper, the contact characteristics of the carbon brush/slip ring of the hydrogenerator under the eccentric vibration of the rotor are studied. The influence of spring parameters on the contact loss of the carbon brush/slip ring was studied by establishing the motion model of the carbon brush/slip ring for theoretical calculation and fitting the motion trajectory curve with MATLAB software. Studies have shown that the loss of contact is mainly related to the spring damping coefficient and the precompression. By optimizing these two parameters, the contact stability of the carbon brush on the ring surface of the slip ring can be improved. It provides a theoretical reference for the design and optimization of the parameters of the carbon brush/slip ring spring.

1. Introduction

Hydrogenerator carbon brushes/slip rings are the key components to guide the excitation current of the hydrogenerators into the rotor windings, and both of them use sliding contact to realize the conduction of current [1]. Carbon brush/slip ring friction pair is a typical sliding friction pair under high current and low contact pressure; under this working condition, the surface contact of the friction pair belongs to a more complex contact model in which electrical contact and mechanical contact are coupled together [2, 3], so the contact stability between the carbon brush and the slip ring has always been a hot issue in engineering application research.

When the hydrogenerators are in operation, due to the eccentric distance between the rotor center of mass and the rotation center, it will produce eccentric vibration when the rotor rotating. Under the influence of this eccentric vibration, the contact force between the carbon brush and the ring surface of the slip ring changes dynamically; under the influence of this dynamic contact force, the contact between the carbon brush and the slip ring surface will be unstable, which will lead to increased vibration and shock and electric-arc discharge in severe cases [4]; this leads to some problems such as carbon brush ignition and tempering which have seriously affected the safe and stable operation of the hydrogenerators.

At present, most of the research studies on the surface contact of carbon brushes and slip rings and the causes of electric-arc generation mainly focus on the contact voltage drop [5, 6] and current density [7, 8]. However, the root cause of arc generation is vibration caused by unstable contact between friction pairs [9] and then transient loss of contact, which is caused by the current breaking through the air [10]; this is directly related to the spring pressure [11]. Argibay [12] studied the asymmetric wear behavior of the brush on the surface of the slip ring and found that even short periods of instability can cause increased brush wear and rapid deterioration of contact resistance and shorter life. Yasar [13] studied the wear characteristics of the spring pressure on the brush and found that when the spring pressure is insufficient, an electric-arc and a higher voltage drop will be generated on the contact surface; the pressure of the spring cannot be too small or too large [14]. There is a suitable range so that the brush can be in stable contact on the ring surface of the slip ring without excessive pressure and increasing the wear of the brush. The increase of pressure within a certain range will effectively improve the system reliability [15].

Therefore, this paper establishes the motion model of the carbon brush/slip ring under the eccentric oscillation of the hydrogenerator rotor, and through calculation, the motion equation of the carbon brush in the eccentric rotation of the

slip ring and the motion equation of the contact point on the slip ring are obtained; then, we use MATLAB software to fit the trajectory curve of the carbon brush and the trajectory curve of the contact point on the slip ring and compare these two curves to analyze the contact dynamic response of the carbon brush/slip ring under the influence of rotor eccentric vibration; the main influencing factor for the loss of contact between the carbon brush and the slip ring is the spring parameter, including spring stiffness, spring damping coefficient, and precompression when the spring is installed; then, we comprehensively analyze the influence of these factors on the dynamic response of the carbon brush/slip ring surface contact. It provides a theoretical reference for parameter optimization design of carbon brush/slip ring friction pair spring.

2. Carbon Brush/Slip Ring Structure and Working Principle

The main components of the carbon brush/slip ring structure of the hydrogenerators include four parts: carbon brush, brush grip, spring, and slip ring; the structure diagram is shown in Figure 1. The slip ring is connected to the rotor through the main shaft of the hydrogenerator; the carbon brush is installed in the brush grip. In order to ensure the flexibility of the carbon brush in the brush grip, the two use gap mates; one end of the carbon brush provides stable pressure through the spring, and the other end is in sliding contact with the ring surface of the slip ring. The bottom end of the brush grip is fixedly installed on the frame of the water turbine generator. A braid is installed at the end of the carbon brush, and the braid is fixed on the brush holder by a fastening screw; the bottom end of the brush holder is equipped with a plastic movable handle, which is convenient to replace the carbon brush with electric disassembly in practical engineering.

When the hydrogenerators are running, the rotor rotates to drive the slip ring to rotate; there are several carbon brushes installed around the slip ring. Carbon brush sliding friction comes in contact with the slip ring surface under the pressure of the spring. With the continued friction and wear, the carbon brush can always maintain stable contact with the ring surface of the slip ring. The excitation current of the hydrogenerator flows through the carbon brushes through the brush braid and then is conducted to the generator rotor winding through the sliding contact of the carbon brush/slip ring [16] to provide the required magnetic field for the generator rotor winding. As a key component of the excitation system of the hydrogenerators, the stability of its operation directly affects the safety and reliability of the whole excitation system, which in turn affects the stable operation of the hydrogenerators.

3. Establishment of the Carbon Brush/Slip Ring Movement Model

3.1. Force Analysis of Carbon Brush. Before carrying out the force analysis, make the following assumptions based on the characteristics of the system. (1) Since the size of the slip ring in the Y direction is much larger than the size of the carbon brush, the vibration in this direction does not affect its contact, so we only consider the vibration in the horizontal direction, the X direction. (2) The carbon brush material is usually electrochemical graphite, which is manufactured by pressing, baking, and other processes [17]. The slip ring is a steel slip ring. Both can be regarded as isotropic materials and both are rigid bodies. (3) Since the carbon brush is regarded as a rigid body, the influence of the carbon powder peeled off during the sliding friction process is not considered. (4) The air, humidity, and oil mist in the slip ring chamber mainly affect its wear characteristics and have little impact on contact. Therefore, the influence of the air, humidity, and oil mist in the slip ring chamber is not considered.

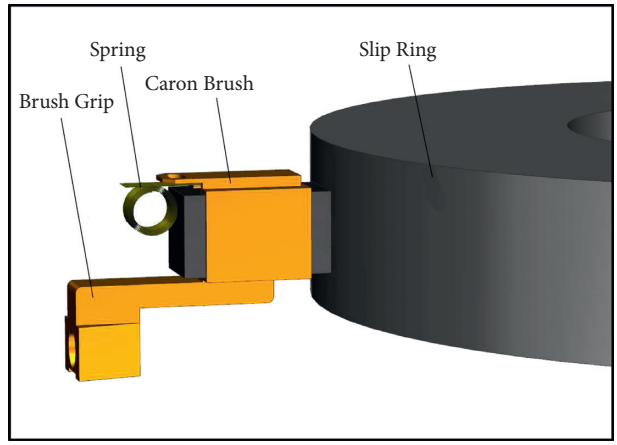

Figure 1: Schematic diagram of the carbon brush/slip ring structure.

According to the movement periodicity of the carbon brush/slip ring system, take one cycle of the slip ring as the research object.

Suppose the carbon brush is deflected in the brush box; the force analysis diagram of the carbon brush is shown in Figure 2(a). It can be seen from the figure that, in the X-axis direction, the carbon brush is subjected to the spring force F_K and the supporting force of the slip ring facing the carbon brush F_{N_1}, and the friction between the carbon brush and the inner wall of the brush box is f_1 and f_1', In the Y-axis direction, it is subjected to the friction force f_2 of the slip ring on it; suppose the deflection angle is α, and the supporting force of the contact surface between the carbon brush and the inner wall of the brush box is, respectively, F_{N_2} and F_{N_3}. Assuming that the slip ring rotates at a constant speed, the carbon brushes make a variable acceleration reciprocating linear motion in the X-axis direction under the premise that the carbon brush and the slip ring are always in good contact. Therefore, when $t \in [0, T/4] \cup [3T/4, T]$,

$$F_K + \mu_1 F_{N_2} \cos\alpha + \mu_1 F_{N_3} \cos\alpha - F_{N_1} = \frac{G_c}{g} a. \tag{1}$$

When $t \in [T/4, 3T/4]$,

$$F_K - \mu_1 F_{N_2} \cos\alpha - \mu_1 F_{N_3} \cos\alpha - F_{N_1} = \frac{G_c}{g} a. \tag{2}$$

In the formula, μ_1 suggests the coefficient of friction between the carbon brush, the inner wall of the brush box G_c

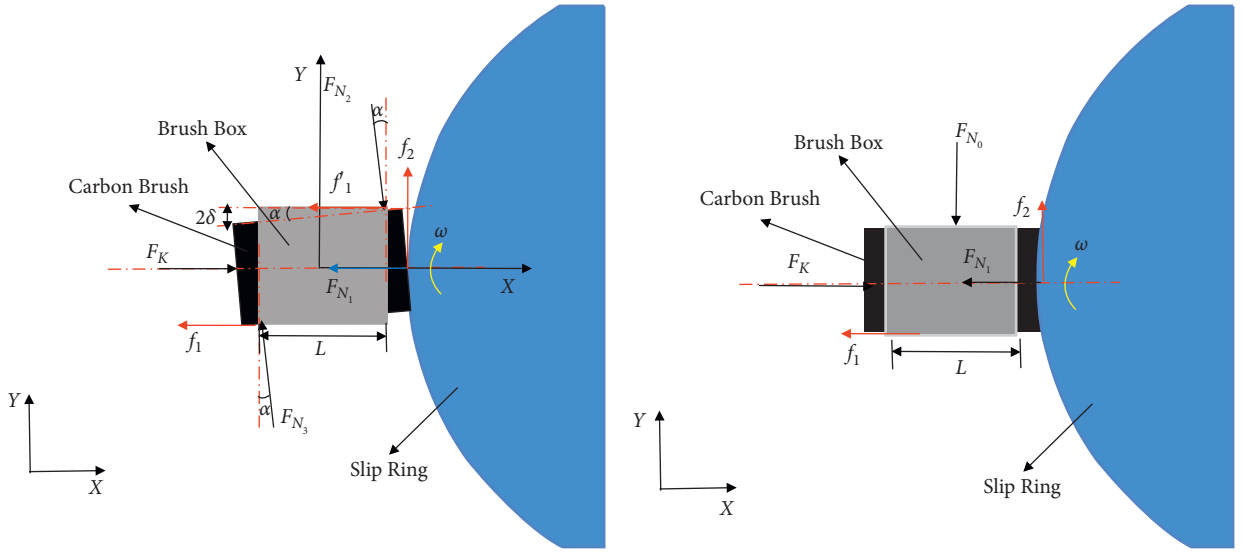

Figure 2: Force diagram of the carbon brush in the contact state.

suggests the carbon brush gravity (N), a suggests the carbon brush acceleration (mm/s^2),

$$F_{N_2} \sin \alpha - F_{N_3} \sin \alpha - f_2 = 0, \tag{3}$$

and α is equal to the angle between the carbon brush and the brush box:

$$\alpha = \sin^{-1} \frac{2\delta}{L}. \tag{4}$$

In the formula, δ suggests the assembly gap between the carbon brush and the brush holder (mm) and L suggests the brush box width (mm).

With the passage of wear time, the contact surface of the carbon brush will gradually form a curved surface with the same curvature as the ring surface of the slip ring after the carbon brushes are in stable contact with the ring surface of the slip ring. At this time, the deflection angle of the carbon brush in the brush box is so small that it can be ignored. Therefore, in this case, the carbon brush does not deflect in the brush box; the force analysis of the carbon brush is shown in Figure 2(b). When $\alpha = 0$, equations (1) and (2) can be simplified as follows.

When $t \in [0, T/4] \cup [3T/4, T]$,

$$F_K + f_1 - F_{N_1} = \frac{G_c}{g} a. \tag{5}$$

When $t \in [T/4, 3T/4]$,

$$F_K - f_1 - F_{N_1} = \frac{G_c}{g} a. \tag{6}$$

Assuming that the average support force of the brush box to the carbon brush is F_{N_0}, then

$$F_{N_0} - f_2 = 0. \tag{7}$$

Friction between the carbon brush and the inner wall of the brush box is

$$f_1 = \mu_1 \left(F_{N_0} + G_c \right). \tag{8}$$

Friction between carbon brush and slip ring:

$$f_2 = \mu_2 F_{N_1}, \tag{9}$$

where μ_2 suggests the friction coefficient between the carbon brush and the slip ring.

From formulas (7)–(9),

$$f_1 = \mu_1 \left(\mu_2 F_{N_1} + G_c \right). \tag{10}$$

Spring force:

$$F_K = K \left(\Delta x + x_0 \right), \tag{11}$$

where K suggests the spring stiffness coefficient (N/mm), Δx suggests the instantaneous deformation of the spring caused by polarization (mm), and x_0 suggests the spring pre-compression (mm).

The instantaneous spring deformation Δx of the spring caused by polarization is a function of the polarization position of the slip ring and is related to the rotation time of the slip ring, which is

$$\Delta x = f(t). \tag{12}$$

Among them,

$$f(t) = \varnothing (1 - \cos \omega t), \tag{13}$$

where ω suggests the angular velocity of slip ring rotation (rad/s) and $\varnothing$ suggests the eccentricity (mm).

Then, the relationship of spring force with time is

$$F_K = K [\varnothing (1 - \cos \omega t) + x_0]. \tag{14}$$

3.2. Motion Analysis of Carbon Brush. Assuming that the carbon brush is always in stable contact with the slip ring, the

positional relationship between the brush and the slip ring is shown in Figure 3. Curve 1 represents the trajectory curve of the center of mass of the slip ring, and Curve 2 represents the trajectory curve of the contact point between the carbon brush and the slip ring. The position of the carbon brush is a function of the corner of the slip ring, that is,

$$x = f(\theta) = \varnothing(1 - \cos\theta). \tag{15}$$

The study found that the carbon brush and the slip ring tend to lose contact when the slip ring is far away from the spring end. This stage is taken as the research object. The spring compression in the initial state is x_0; that is, the spring pressure at point A in Figure 4:

$$F_{K_A} = Kx_0, \tag{16}$$

When the slip ring rotates eccentrically for $T/4$ cycles, the carbon brush moves to point B in Figure 4. At this time, the displacement of the carbon brush is $\varnothing = \omega T/4$, that is, the compression amount of the spring is $x_0 + \omega T/4$; the spring pressure becomes

$$F_{K_B} = K\left(x_0 + \frac{\omega T}{4}\right). \tag{17}$$

When the slip ring rotates eccentrically for $3T/4$ cycles, the carbon brush moves to point C in Figure 4. At this time, the displacement of the carbon brush is $-\varnothing = -3\omega T/4$, that is, the compression amount of the spring is $x_0 - 3\omega T/4$; the spring pressure becomes

$$F_{K_C} = K\left(x_0 - \frac{3\omega T}{4}\right). \tag{18}$$

During the process from B to C, the trajectory of the carbon brush is shown in Figure 4. Due to the influence of the spring resistance, the spring force is gradually reduced. Set the spring damping coefficient to γ, the resistance is proportional to the movement speed, and the direction is opposite to the speed direction. Suppose the resistance is f_T and the speed is v; then,

$$f_T = \gamma v. \tag{19}$$

Taking the spring-carbon brush system as the research object and assuming that the displacement of the carbon brush at any moment in the process of moving from position B to position C is x and the speed is v in Figure 3, then, at this time, the compression of the spring is $x_0 + \varnothing - x$, and the spring pressure is

$$F_{K_0} = K(x_0 + \varnothing - x). \tag{20}$$

Then, the initial carbon brush speed v_0 is

$$v_0 = \frac{F_{K_0} - F_{N_1}}{\gamma} = \frac{K(x_0 - x) - F_{N_1}}{\gamma}. \tag{21}$$

During this process, the carbon brush performs a variable acceleration linear motion. In the initial state, the initial speed of the carbon brush is $v_0 = 0$, and the displacement of the carbon brush $x = 0$; then,

$$\frac{Kx_0 - F_{N_1}}{\gamma} = 0. \tag{22}$$

We can solve

$$F_{N_1} = Kx_0. \tag{23}$$

It is assumed that the counterforce of the slip ring to the carbon brush is always constant. According to Newton's law of motion,

$$F_{K_0} - f_T - f_1 = \frac{G_c}{g} \cdot \frac{dv}{dt}, \tag{24}$$

which is

$$K(x_0 + \varnothing - x) - \gamma V - \mu_1\left(\mu_2 F_{N_1} + G_c\right) = \frac{G_c}{g} \cdot \frac{dv}{dt}. \tag{25}$$

The differential equation of carbon brush movement is

$$\frac{G_c}{g}\frac{d^2x}{dt^2} = K(x_0 + \varnothing - x) - \gamma\frac{dx}{dt} - \mu_1(\mu_2 Kx_0 + G_c). \tag{26}$$

So, deforming the above formula, we concluded

$$\frac{d^2x}{dt^2} + \frac{\gamma g}{G_c}\frac{dx}{dt} + \frac{Kg}{G_c}x = \frac{Kg}{G_c}(x_0 + \varnothing) - \frac{\mu_1 g}{G_c}(\mu_2 Kx_0 + G_c), \tag{27}$$

We can get the characteristic equation as

$$\lambda^2 + \frac{\gamma g}{G_c}\lambda + \frac{Kg}{G_c} = 0. \tag{28}$$

Solve the characteristic root as

$$\begin{aligned}\lambda &= \frac{-\gamma g/G_c \pm \sqrt{(\gamma g/G_c)^2 - 4Kg/G_c}}{2} \\ &= \frac{-\gamma g \pm \sqrt{(\gamma g)^2 - 4KgG_C}}{2G_c}.\end{aligned} \tag{29}$$

The general solution of the differential equation is

$$x = C_1 e^{\lambda_1 t} + C_2 e^{\lambda_2 t}. \tag{30}$$

Among them, C_1 and C_2 are both constants.

Suppose the special solution of this differential equation is $x = b_0$. Substituting formula (27),

$$b_0 = x_0 + \varnothing - \frac{\mu_1}{K}(\mu_2 Kx_0 + G_c). \tag{31}$$

Therefore, the general solution of the differential equation is

$$x = C_1 e^{\lambda_1 t} + C_2 e^{\lambda_2 t} + x_0 + \varnothing - \frac{\mu_1}{K}(\mu_2 Kx_0 + G_c). \tag{32}$$

The speed v of the carbon brush is

$$v = \frac{dx}{dt} = C_1\lambda_1 e^{\lambda_1 t} + C_2\lambda_2 e^{\lambda_2 t}, \tag{33}$$

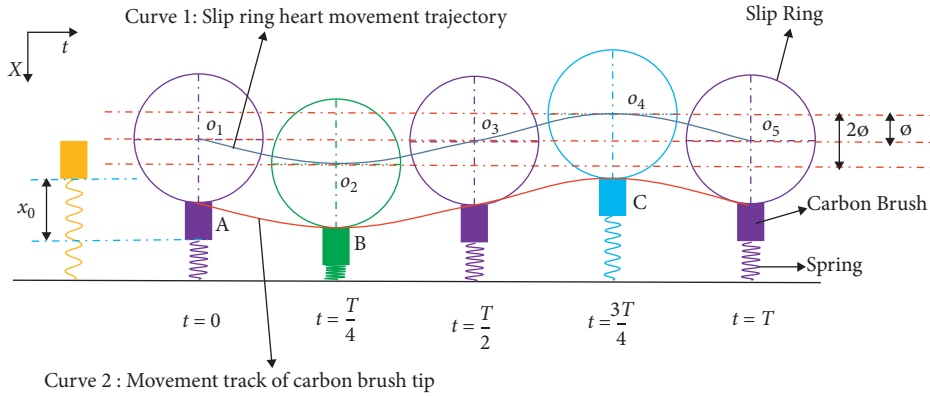

Figure 3: Schematic diagram of spring compression in $T/2$ cycles.

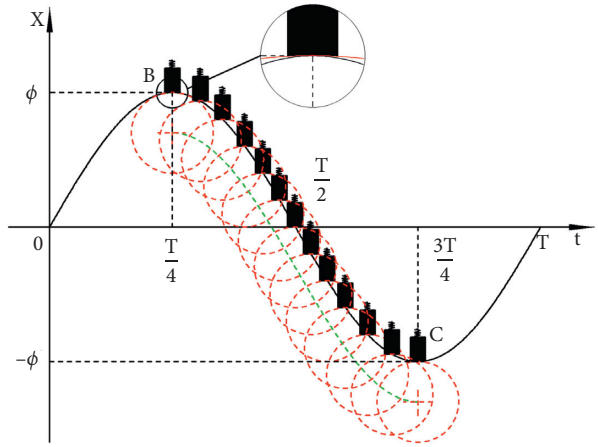

Figure 4: Carbon brush running track diagram in $T/2$ cycle.

where $\lambda_1 = -\gamma g + \sqrt{(\gamma g)^2 - 4KgG_C/2G_c}$ and $\lambda_2 = -\gamma g - \sqrt{(\gamma g)^2 - 4KgG_C/2G_c}$.

In the initial state, that is when the carbon brush is at point B in Figure 4, $t = 0$, $v = 0$, and $x = -\varnothing$; substituting formulas (32) and (33),

$$C_1 + C_2 + x_0 + \varnothing - \frac{\mu_1}{K}(\mu_2 K x_0 + G_c) = -\varnothing, \tag{34}$$

$$C_1\lambda_1 + C_2\lambda_2 = 0. \tag{35}$$

Combining solutions (34) and (35), we can obtain

$$C_1 = \frac{[x_0 - \mu_1/K(\mu_2 K x_0 + G_c) + 2\varnothing]\lambda_2}{\lambda_1 - \lambda_2},$$
$$C_2 = \frac{[\mu_1/K(\mu_2 K x_0 + G_c) - x_0 - 2\varnothing]\lambda_1}{\lambda_1 - \lambda_2}. \tag{36}$$

Substituting C_1 and C_2 into formula (32), we can get the equation of motion of the carbon brush as

$$x = \frac{[x_0 - \mu_1/K(\mu_2 K x_0 + G_c) + 2\varnothing]\lambda_2}{\lambda_1 - \lambda_2} e^{\lambda_1 t} - \frac{[x_0 - \mu_1/K(\mu_2 K x_0 + G_c) + 2\varnothing]\lambda_1}{\lambda_1 - \lambda_2} e^{\lambda_2 t} + x_0 + \varnothing - \frac{\mu_1}{K}(\mu_2 K x_0 + G_c). \tag{37}$$

When the research system is clear, generally, μ_1, μ_2, K, x_0, G_c, and $\varnothing$ are constant, so assuming $x_0 + \varnothing - \mu_1/K(\mu_2 K x_0 + G_c) = \eta$, the carbon brush motion equation can be simplified as

$$x = \frac{(\eta + \varnothing)\lambda_2}{\lambda_1 - \lambda_2} e^{\lambda_1 t} - \frac{(\eta + \varnothing)\lambda_1}{\lambda_1 - \lambda_2} e^{\lambda_2 t} + \eta. \tag{38}$$

3.3. Judgment of Loss of Contact between Carbon Brush and Slip Ring. When the carbon brush loses contact with the slip ring, the force analysis of the carbon brush is shown in Figure 5. At this time, $F_N = 0$; the carbon brush is only subjected to the spring force F_K and the friction force f_1 of the inner wall of the brush box, and the carbon brush makes a linear motion in the X-axis direction with variable acceleration.

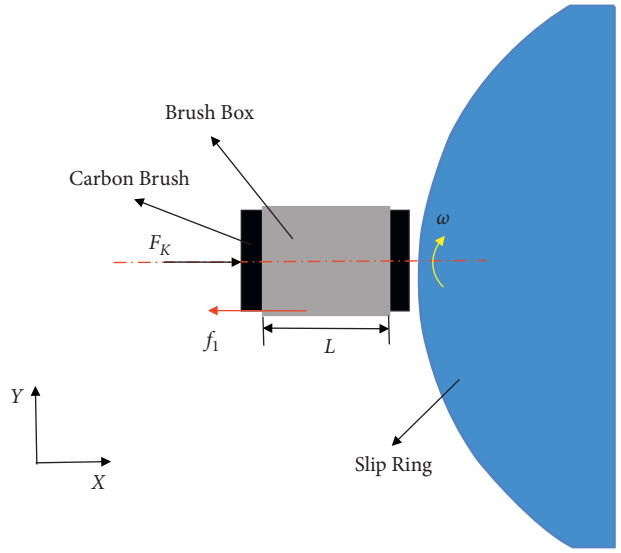

Figure 5: Force diagram of the carbon brush under loss of contact.

Taking the contact points on the torus of the slip ring as the research object, its trajectory in one cycle is shown in Figure 6, and the time period from B to C in the figure is taken as the research object, so its motion equation at this stage is

$$X = \varnothing \cos \omega t. \tag{39}$$

Suppose the rotation speed of the slip ring is V, the radius is r, and the time for one revolution is t, so the rotation period T is

$$T = t = \frac{2\pi r}{V'} = \frac{2\pi}{\omega}. \tag{40}$$

Among the parameters of the carbon brush and the slip ring, G_c, V, r, $\varnothing$, μ_1, and μ_2 can be regarded as fixed parameters; K, γ, and x_0 are spring parameters, which are optimizable parameters and regarded as variable parameters. Relying on the actual working conditions and the actual operating parameters of the carbon brushes/slip rings of the power plant, the fixed parameters of the carbon brushes/slip rings are shown in Table 1.

Substituting these known parameters into formula (37), we can get the equation of motion of the carbon brush as (the acceleration of gravity $g = 10\text{m/s}^2$)

$$\begin{aligned} x = {} & \frac{[x_0 - 0.3/K(0.3Kx_0 + 1) + 2]\lambda_2}{\lambda_1 - \lambda_2} e^{\lambda_1 t} \\ & - \frac{[x_0 - 0.3/K(0.3Kx_0 + 1) + 2]\lambda_1}{\lambda_1 - \lambda_2} e^{\lambda_2 t} + x_0 + 1 \\ & - \frac{0.3}{K}(0.3Kx_0 + 1). \end{aligned} \tag{41}$$

According to the actual parameters of the carbon brush/slip ring spring of a power station, the spring parameters are shown in Table 2.

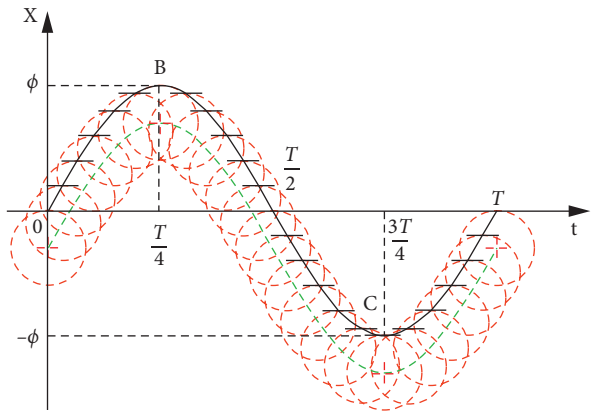

Figure 6: Running track diagram of the slip ring in one cycle.

Substituting the spring parameters into formula (41), we can get the equation of motion of the carbon brush as

$$x = \frac{2.85}{10\sqrt{2}}\left[(10 - 5\sqrt{2})e^{(-10-5\sqrt{2})t} - (5\sqrt{2} + 10)e^{(5\sqrt{2}-10)t}\right] + 1.85. \tag{42}$$

The motion equation of the contact point on the slip ring can be expressed as

$$X = \cos\frac{3467}{530}t. \tag{43}$$

The time T for the slip ring to make one revolution is

$$T = \frac{2\pi r}{V'} = \frac{1060\pi}{3467}. \tag{44}$$

According to the motion equation of the carbon brush and the motion equation of the contact point on the slip ring, the trajectory of the carbon brush and the contact point on the slip ring in a period can be drawn, respectively, as shown in Figure 7. Curve 1 represents the trajectory of the carbon

Table 1: Carbon brush/slip ring fixed parameter table.

Parameter name	
Carbon brush gravity (N)	1
Slip ring speed (mm/s)	3467
Slip ring radius (mm)	530
Rotor eccentricity (mm)	1
Coefficient of friction between the carbon brush and the inner wall of the brush holder	0.3
Friction coefficient between the carbon brush and the slip ring	0.3

Table 2: Spring preset parameter table.

Parameter name	
Spring stiffness (N/mm)	5
Spring damping coefficient	2
Spring precompression (mm)	1

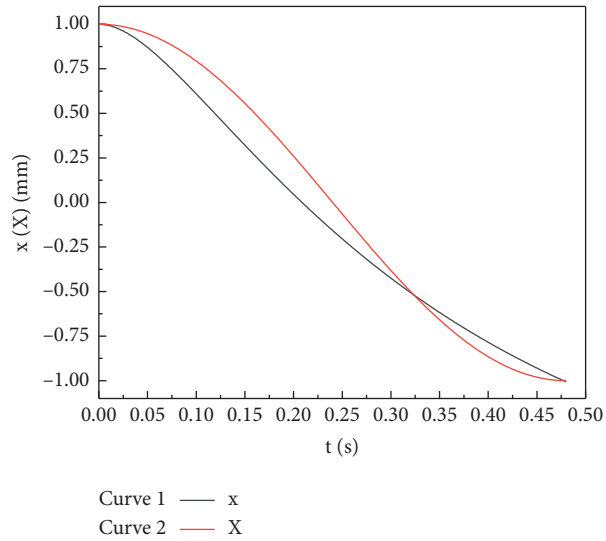

Figure 7: Running track diagram of the carbon brush and the slip ring in one cycle.

brush during this period. Curve 2 represents the trajectory of the contact point on the slip ring in this period.

By comparing the movement trajectory of the carbon brush with the movement trajectory of the contact point on the slip ring in a cycle, it can be judged whether the carbon brush and the slip ring have lost contact. If the trajectory of the carbon brush is always below or coincides with the trajectory of the contact point on the slip ring, it means that, in this process, the displacement of the carbon brush without the reaction force of the ring surface of the slip ring is always greater than or equal to the displacement of the contact point on the slip ring. It means that there is no loss of contact between the carbon brush and the slip ring during this process. If the trajectory of the carbon brush is above the trajectory of the contact point on the slip ring within a certain period of time, it means that the carbon brush and the slip ring have lost contact during this period of time. It can be seen from Figure 7 that the carbon brush and the slip ring start to lose contact in 0.3 seconds.

The displacement difference between the carbon brush and the slip ring, that is, the straight distance between the two curves, can be expressed as

$$\xi = x - X = \frac{2.85}{10\sqrt{2}}\left[(5\sqrt{2}-10)e^{(-10-5\sqrt{2})t} - (5\sqrt{2}+10)e^{(5\sqrt{2}-10)t}\right] + 1.85 - \cos\frac{3467}{530}t. \tag{45}$$

Among them, the time $t \in (0, T)$, as can be seen from the movement characteristics of the carbon brush and the slip ring; the loss of contact mainly occurs during the time period when the slip ring is away from the spring end, that is, $t \in (0, T)$. In the time period, the four time points are evenly taken in this time period as at $T/8$, $T/4$, $3T/8$, and $T/2$; we study the influence of spring parameters on ξ at these four times and draw a graph of the relationship between spring parameters and ξ.

It can be seen that if $\xi = x - X \leq 0$, it means that there is no loss of contact between the carbon brush and the slip ring. Otherwise, if $\xi = x - X > 0$, it means that the carbon brush has lost contact with the slip ring. Therefore, the spring parameters can be optimized by using ξ as the optimization target. The relationship diagram of ξ with time t is shown in Figure 8. It can be seen from the figure that $\xi > 0$ between 0.3 s and 0.5 s indicates that the carbon brush and the slip ring have lost contact during this time period.

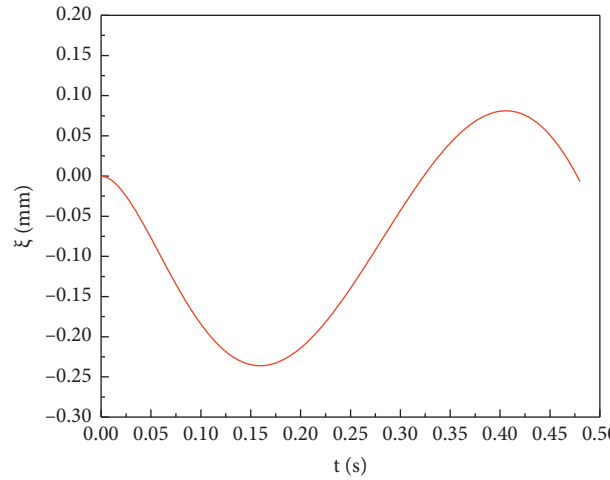

Figure 8: The relationship between the displacement differences between the carbon brush and the slip ring with respect to time.

4. Analysis of Contact Dynamic Response Characteristics

4.1. Factors Affecting Loss of Contact. Due to the difference in stiffness and damping coefficient of the spring, its rebound time after being compressed is also different. We call this rebound time the response time of the spring. If the response time is too long, the carbon brush will lose contact with the slip ring and will be affected by the eccentricity of the rotor.

It can be seen from the motion equation of the carbon brush that the motion of the carbon brush is related to the following parameters: $\mu_1, \mu_2, K, x_0, \gamma$, and G_c. Among them, μ_1, μ_2, and G_c are predetermined parameters, which are only related to the material properties of the brush holder, the slip ring, and the carbon brush. Therefore, the main factors affecting the loss of contact between the carbon brush and the slip ring are the spring parameters, namely, K, γ, and x_0. In order to obtain the influence of the three factors on the loss of contact of the carbon brush/slip ring, the control variables are used to study the influence of K, γ, and x_0 on the loss of contact.

(1) Control γ and x_0 are to be constant; we take $\gamma = 2$ and $x_0 = 1$mm; at this time, the displacement difference between the carbon brush and the slip ring can be expressed as

$$\xi = \frac{[3 - 0.3/K(0.6K + 1)]\lambda_2}{\lambda_1 - \lambda_2} e^{\lambda_1 t} - \frac{[3 - 0.3/K(0.6K + 1)]\lambda_1}{\lambda_1 - \lambda_2} e^{\lambda_2 t} + 2 - \frac{0.3}{K}(0.6K + 1) - \cos\frac{3467}{530}t, \quad (46)$$

where $\lambda_1 = -20 + \sqrt{400 - 40K}/2$ and $\lambda_2 = -20 - \sqrt{400 - 40K}/2$.

Respectively, we take $t = T/8 = 265\pi/6934$, $t = T/4 = 265\pi/3467$, $t = 3T/8 = 795\pi/6934$, and $t = T/2 = 530\pi/3467$; within the allowable range $K\epsilon$ (1 N/mm, 10 N/mm), we change K to get the relationship curve between K and ξ, as shown in Figure 9.

(2) Control K and x_0 are to be constant; we take $K =$ 5N/mm and $x_0 = 1$mm; at this time, the displacement difference between the carbon brush and the slip ring can be expressed as

$$\xi = \frac{2.85\lambda_2}{\lambda_1 - \lambda_2} e^{\lambda_1 t} - \frac{2.85\lambda_1}{\lambda_1 - \lambda_2} e^{\lambda_2 t} + 1.85 - \cos\frac{3467}{530}t, \quad (47)$$

where $\lambda_1 = -10\gamma + \sqrt{(10\gamma)^2 - 200}/2$ and $\lambda_2 = -10\gamma - \sqrt{(10\gamma)^2 - 200}/2$.

Respectively, we take $t = T/8 = 265\pi/6934$, $t = T/4 = 265\pi/3467$, $t = 3T/8 = 795\pi/6934$, and $t = T/2 = 530\pi/3467$, within the allowable range $\gamma\varepsilon(1, 5)$. We change γ to obtain the relationship curve between γ and ξ, as shown in Figure 10.

(3) Control K and γ are to be constant; we take $K =$ 5N/mm and $\gamma = 2$; at this time, the displacement difference between the carbon brush and the slip ring can be expressed as

$$\xi = \frac{(0.91x_0 + 1.94)\lambda_2}{\lambda_1 - \lambda_2} e^{\lambda_1 t} - \frac{(0.91x_0 + 1.94)\lambda_1}{\lambda_1 - \lambda_2} e^{\lambda_2 t} + 0.91x_0 + 0.94 - \cos\frac{3467}{530}t. \quad (48)$$

In the formula, $\lambda_1 = -10 + 5\sqrt{2}$ and $\lambda_2 = -10 - 5\sqrt{2}$.

Respectively, we take $t = T/8 = 265\pi/6934$, $t = T/4 = 265\pi/3467$, $t = 3T/8 = 795\pi/6934$, and $t = T/2 = 530\pi/3467$, within the allowable range $x_0\epsilon$ (0 mm, 5 mm). We change x_0 to get a graph of the relationship between x_0 and ξ, as shown in Figure 11.

In the three figures, curve 1, curve 2, curve 3, and curve 4, respectively, represent the relationship curves of K, γ, x_0, and ξ when the time is $T/8$, $T/4$, $3T/8$, and $T/2$.

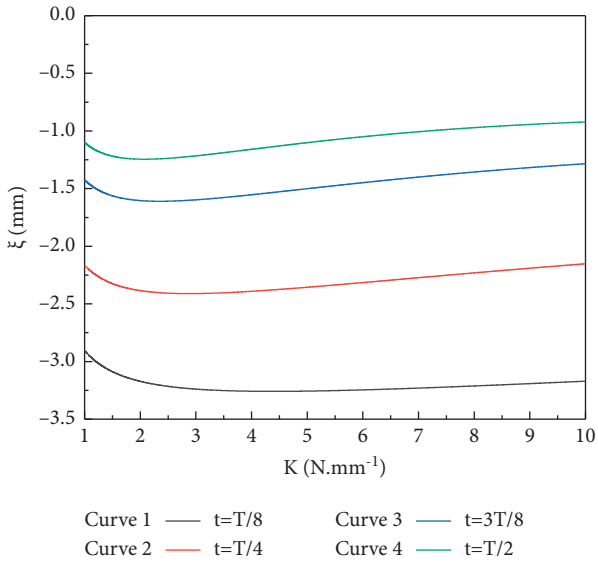

Figure 9: The relationship curve between spring stiffness K and ξ.

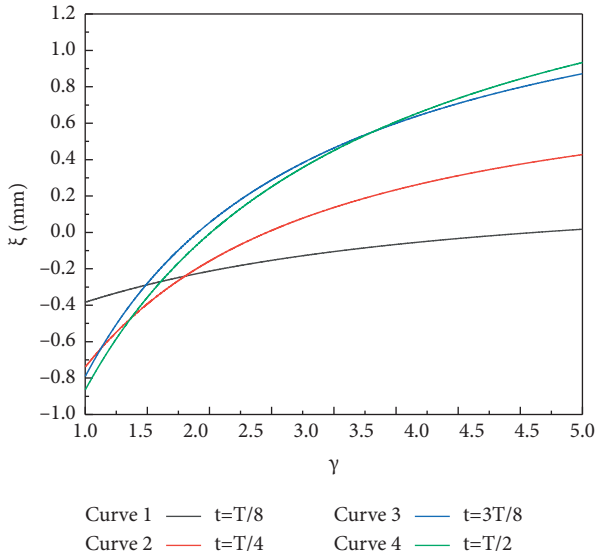

Figure 10: The relationship curve diagram of spring damping coefficient γ and ξ.

It can be seen from Figure 9 that, with the increase of K, the displacement difference ξ between the carbon brush and the slip ring first decreases and then increases and is always less than 0. This shows that the carbon brush and the slip ring will not lose contact under the influence of the rotor eccentric vibration.

It can be seen from Figure 10 that, with the increase of γ, the displacement difference ξ between the carbon brush and the slip ring gradually increases, and when γ approaches positive infinity, ξ must be more than 0, which means that, as the spring damping coefficient increases, the carbon brushes and the slip ring will lose contact under the influence of the rotor eccentricity. It can be seen from the figure that when $t = T/2$ and $\gamma \le 2.0$, $\xi \le 0$; it means that, under the premise of certain other parameters, when $\gamma \le 2.0$, the carbon brush and the slip ring will not lose contact under the influence of the eccentric vibration of the rotor.

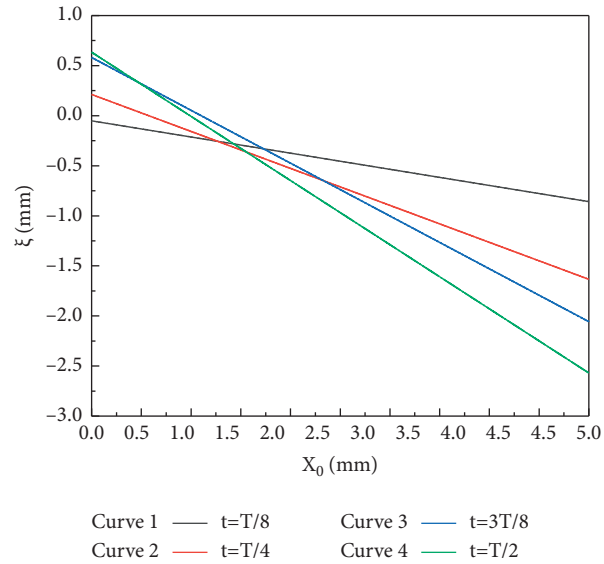

Figure 11: The relationship curve between spring precompression x_0 and ξ.

It can be seen from Figure 11 that, as x_0 increases, the displacement difference ξ between the carbon brush and the slip ring gradually decreases. When $t = T/4$ and $x_0 \ge 0.7$ mm, $\xi \le 0$; when $t = 3T/8$ and $x_0 \ge 1.25$ mm, $\xi \le 0$; when $t = T/2$ and $x_0 \ge 1.2$ mm, $\xi \le 0$; it means that, under the premise of certain other parameters, when $x_0 \ge 1.25$ mm, the carbon brush and the slip ring will not lose contact under the influence of the eccentric vibration of the rotor.

4.2. Case Study. Take a hydrogenerator of a hydropower station as an example; the carbon brush did not lose contact with the ring surface of the slip ring during a period of operation. The length of the carbon brush changed by 2.5 mm after abrasion measured on-site. The precompression amount set when the spring was installed was 5 mm, and the compression amount of the spring after wear becomes 2.5 mm. The specific parameters are shown in Table 3. According to the calculation of the above theoretical formula, the movement trajectory curve of the carbon brush before and after wear and the movement trajectory curve of the contact point on the collector ring are obtained, respectively, as shown in Figure 12. It can be seen from the figure that the displacement of the carbon brushes before and after wear is always greater than the displacement of the contact point on the slip ring; this shows that there is no loss of contact between the carbon brush and the slip ring under the influence of the rotor eccentricity. The theoretical calculation results are consistent with the actual case.

Because the most important factor that affects the loss of contact between the carbon brush and the slip ring is the spring parameter, therefore, in order to ensure the stable contact between the carbon brush and the slip ring during the operation of the hydrogenerators, we can optimize the

Table 3: Carbon brush/slip ring parameter table.

Parameter name		Remarks
Carbon brush gravity (N)	1	D172 carbon brush
Slip ring speed (mm/s)	3467	
Slip ring radius (mm)	530	
Rotor eccentricity (mm)	1	
Coefficient of friction between the carbon brush and the inner wall of the brush holder	0.3	
Friction coefficient between carbon brush and slip ring	0.3	
Spring stiffness (N/mm)	2	
Spring damping coefficient	1	
Spring precompression (mm)	5	
Spring compression after carbon brush wear (mm)	2.5	

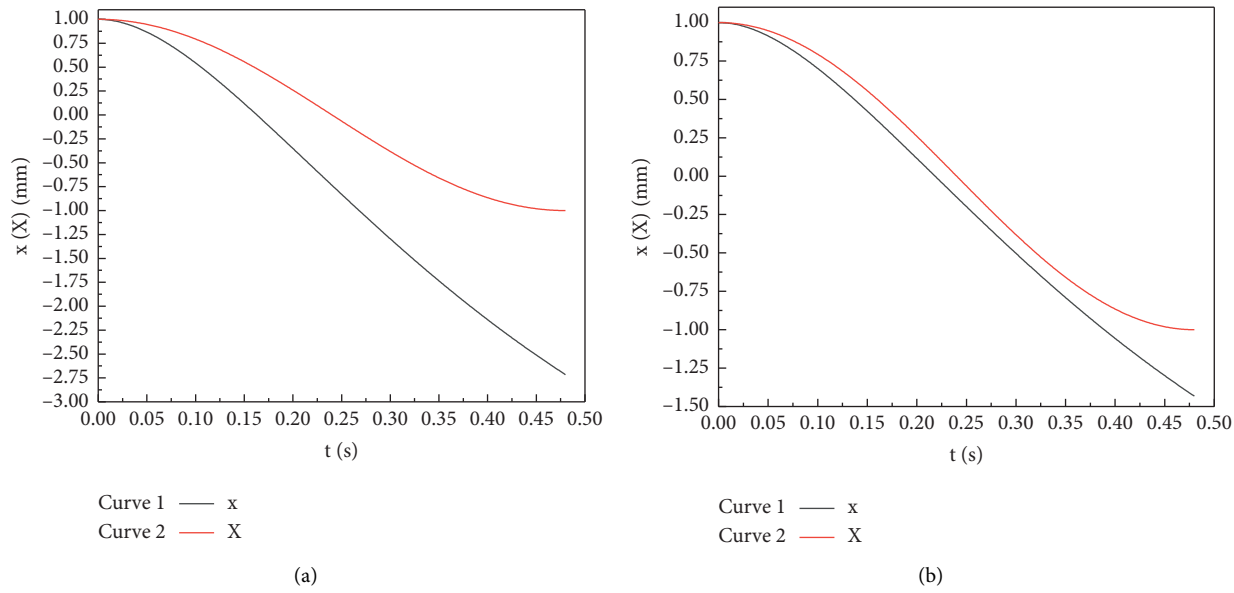

Figure 12: Running track diagram of carbon brush and slip ring during half cycle before and after abrasion.

parameters from the spring parameters. According to the calculation results of the above theoretical formulas, the influence of each spring parameter on the surface contact characteristics of the carbon brush/slip ring can be judged, and the spring parameters can be optimized accordingly.

4.3. Optimization of Spring Parameters. The contact stability of the carbon brush and the slip ring directly affects its contact stress and contact resistance. When the slip ring rotates, it will drive the surface air to rotate together. When there is a gap between the carbon brush and the slip ring, the rotating air will enter to form a layer of air cushion, which increases the contact resistance between the carbon brush and the slip ring. In order to solve this problem, the contact stability of the carbon brush and the slip ring can be improved by adjusting the spring pressure [18].

The spring is composed of thin steel sheets crimped into multiple concentric circles. The pressure can be adjusted according to the number of turns [19]. In addition, the thickness of the steel sheet will affect the stiffness and damping coefficient of the spring. Therefore, the pressure, stiffness, and damping coefficient of the spring can be adjusted by changing the number of turns and the thickness of the steel sheet. The material of the spring is usually 2Cr19Ni9Mo; different materials have different pressures to the same limit. Therefore, the pressure, stiffness, and damping coefficient can be adjusted by changing the spring material. For any carbon brush/slip ring system of a hydrogenerators, its structural parameters μ_1, μ_2, V, r, G_c, and $\varnothing$ are all known constant parameters; when these parameters are known, the relationship between the surface contact characteristics of the carbon brush/slip ring and the spring parameters can be calculated according to the above formula:

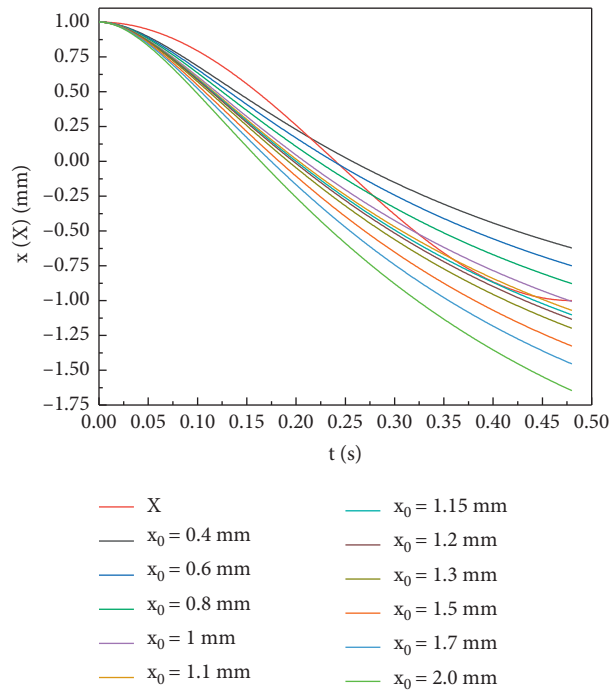

Figure 13: The running track diagram of the carbon brush when the precompression is 0.4 mm~2 mm.

$$\xi = \frac{[x_0 - 0.3/K(0.3Kx_0 + 1) + 2]\lambda_2}{10\sqrt{\gamma^2 - 2}} e^{(-5\gamma+5\sqrt{\gamma^2-2})t} - \frac{[x_0 - 0.3/K(0.3Kx_0 + 1) + 2]\lambda_1}{10\sqrt{\gamma^2 - 2}} e^{(-5\gamma+5\sqrt{\gamma^2-2})t} + x_0 + 1 - \frac{0.3}{K}(0.3Kx_0 + 1) - \cos\frac{3467}{530}t. \tag{49}$$

If the spring material and structural parameters are determined, substituting the spring stiffness and damping coefficient into formula (49), the relationship between surface contact characteristics and precompression can be obtained. Therefore, the contact stability between the carbon brush and the ring surface of the slip ring can be improved by adjusting the amount of precompression. The amount of precompression can be adjusted by changing the installation position of the spring on the brush holder.

Optimize the spring parameters according to the preset parameters in Tables 1 and 2. Because spring stiffness and damping coefficient are spring structure parameters, which are related to its material and size. However, once the material and size of the spring are determined, its stiffness and damping coefficient remain unchanged. Therefore, in actual engineering, the precompression of the spring is usually adjusted to change the surface contact stability of the carbon brush and the slip ring. Substitute the spring structure parameters into formula (38). The relationship between the displacement of the carbon brush and the precompression of the spring is

$$x = \frac{0.91x_0 + 1.94}{10\sqrt{2}}\left[(10 - 5\sqrt{2})e^{(-10-5\sqrt{2})t} - (5\sqrt{2} + 10)e^{(5\sqrt{2}-10)t}\right] + 0.91x_0 + 0.94. \tag{50}$$

Figure 7 is the movement track diagram of the carbon brush when the spring precompression is 1 mm. It can be seen that the carbon brush has lost contact with the annular surface of the slip ring at this time. Adjust the amount of precompression by changing the installation position of the spring. Figure 13 shows the motion trajectory of the carbon brush when taking 0.4 mm to 2 mm for the precompression amount. Combining Figures 11 and 13, it can be seen that when the precompression amount is adjusted to 1.2 mm, the carbon brush and the slip ring will not lose contact. Therefore, to ensure stable contact between the carbon brush and the ring surface of the slip ring under these parameters, combined with the amount of wear of the carbon brush after a period of wear, the precompression of the spring needs to be adjusted above 1.2 mm. In engineering applications, we can use this method to adjust the precompression of the

spring under the premise that the system structural parameters are determined to improve the contact stability of the carbon brush and the slip ring.

5. Conclusions

By establishing the mechanical model and the movement model of the carbon brush/slip ring of the hydrogenerator and combined with the comparative analysis of the movement trajectory curve of the carbon brush/slip ring, it is concluded that

(1) Considering that the shape of the wear surface of the carbon brush/slip ring is the same, when the force of the carbon brush is analyzed, the model can be simplified as the situation when the carbon brush does not deflect in the brush box.

(2) The contact between the carbon brush/slip ring is related to these parameters: μ_1, μ_2, G_c, $\varnothing$, K, γ, and x_0.

(3) The loss of contact between the carbon brush/slip ring is mainly related to the spring parameters K, γ, and x_0. The stability of the contact between the carbon brush/slip ring can be improved by optimizing the spring parameters.

(4) When the spring structure and size are determined, the safety range of the precompression amount is calculated, and the carbon brush wear condition is combined to guide the installation of the carbon brush and the pressure adjustment in the actual project. In addition, the stiffness and damping coefficient of the spring are related to the material of the spring, the thickness of the spring steel leaf, and the number of turns. The calculation results can guide the selection and design of the spring.

Data Availability

The data used to support the findings of this study are available from the corresponding author upon reasonable request.

Conflicts of Interest

The authors declare that they have no conflicts of interest.

References

[1] D. Poljanec, M. Kalin, and L. Kumar, "Influence of contact parameters on the tribological behaviour of various graphite/graphite sliding electrical contacts," *Wear*, vol. 406-407, pp. 75–83, 2018.

[2] L. Huiyang, T. Yan, L. Du, and L. Zhou, "Current situation and prospects of current-carrying friction and wear research," *Materials Guide*, vol. 33, no. 13, pp. 2272–2280, 2019.

[3] H. Xi, P. He, S. Liu, G. Ma, H. Wang, and Z. Lv, "Research status and prospects of conductive wear-resistant self-lubricating coatings," *Surface Technology*, vol. 48, no. 7, pp. 353–363, 2019.

[4] Y. Y. Zhang, Y. Z. Zhang, S. M. Du, C. F. Song, Z. H. Yang, and B. Shangguan, "Tribological properties of pure carbon strip affected by dynamic contact force during current-carrying sliding," *Tribology International*, vol. 123, pp. 256–265, 2018.

[5] J. M. Casstevens, H. G. Rylander, and Z. Eliezer, "Influence of high velocities and high current densities on the friction and wear behavior of copper-graphite brushes," *Wear*, vol. 48, no. 1, pp. 121–130, 1978.

[6] P. Lee and J. Johnson, "High-current brushes, part II: effects of gases and hydrocarbon vapors," *IEEE Transactions on Components, Hybrids, and Manufacturing Technology*, vol. 1, no. 1, pp. 40–45, 1978.

[7] T. Ueno, K. Kadono, S. Yamaguchi, M. Aoyagi, A. Tanaka, and N. Morita, "Relationship between contact voltage drop and frictional coefficient under high-current sliding contact," *IEEJ Transactions on Electrical and Electronic Engineering*, vol. 5, no. 4, pp. 486–492, 2010.

[8] T. A. Dow and J. W. Kannel, "Thermomechanical effects in high current density electrical slip rings," *Wear*, vol. 79, no. 1, pp. 93–105, 1982.

[9] H. Yang, G. Chen, S. Zhang, and W. Zhang, "Effect of the vibration on friction and wear behavior between the carbon strip and copper contact wire pair," *Proceedings of the Institution of Mechanical Engineers-Part J: Journal of Engineering Tribology*, vol. 226, no. 8, pp. 722–728, 2012.

[10] D. K. Lawson and T. A. Dow, "The sparking and wear of high current density electrical brushes," *Wear*, vol. 102, no. 1-2, pp. 105–125, 1985.

[11] T. Ding, G. X. Chen, M. H. Zhu, W. H. Zhang, and Z. R. Zhou, "Influence of the spring stiffness on friction and wear behaviours of stainless steel/copper-impregnated metallized carbon couple with electrical current," *Wear*, vol. 267, no. 5-8, pp. 1080–1086, 2009.

[12] N. Argibay, J. A. Bares, and W. G. Sawyer, "Asymmetric wear behavior of self-mated copper fiber brush and slip-ring sliding electrical contacts in a humid carbon dioxide environment," *Wear*, vol. 268, no. 3-4, pp. 455–463, 2010.

[13] I. Yasar, A. Canakci, and F. Arslan, "The effect of brush spring pressure on the wear behaviour of copper-graphite brushes with electrical current," *Tribology International*, vol. 40, no. 9, pp. 1381–1386, 2007.

[14] J. Du, C. Zhang, and Y. He, "Heating analysis and pressure test of carbon brush slip ring for excitation of hydro-generator," *Journal of Liaoning University of Petroleum & Chemical Technology*, vol. 37, no. 6, pp. 40–43, 2017.

[15] N. Morita, T. Ueno, T. Otaka, and M. Arata, "Comparison of Brush dynamic operation characterisitics for turbine generator steel collector ring," in *Proceedings of the Electrical Contacts-2007 53rd IEEE Holm Conference on Electrical Contacts*, pp. 205–210, Pittsburgh, PA, USA, September 2007.

[16] K. Johan, H. Ohma, and M. Runde, "Wear rates and current distribution of carbon brushes on steel slip rings," *IEEE Transactions on Energy Conversion*, vol. 24, no. 4, pp. 835–840, 2009.

[17] X. Jin-tong, H. Zhong-liang, C. Zhen-hua, and D. Guo-yun, "Preparation of carbon brushes with thermosetting resin binder," *Transactions of Nonferrous Metals Society of China*, vol. 17, no. 6, pp. 1379–1384, 2007.

[18] M. Tong, "Causes of overheating of brush wires of high-speed slip ring of turbo-generators and its improvement measures," *Journal of Electrical Engineering Technology*, vol. 4, p. 49, 1987.

[19] Y. Chen, D. Wang, and J. Wang, "The use and failure analysis of the slip ring and brush holder," *Explosion-proof Motor*, vol. 47, no. 3, pp. 34–36, 2012.